

# Search for extra dimensions at LHC

Laurent Vacavant, for the ATLAS and CMS Collaborations

Lawrence Berkeley National Laboratory, Physics Division, Berkeley CA 94720, USA

Received: 10 October 2003 / Accepted: 24 October 2003 /  
 Published Online: 30 October 2003 – © Springer-Verlag / Società Italiana di Fisica 2003

**Abstract.** Some of the studies performed by the ATLAS and CMS collaborations to establish the future sensitivity of the experiments to extra dimension signals are reviewed. The discrimination of those signals from other new physics signals and the extraction of the underlying parameters of the extra dimension models are discussed.

## 1 Introduction

Models with extra dimensions (ED) (see [1]) are very attractive extensions of the Standard Model (SM), in particular with respect to the hierarchy problem. While ED have so far escaped detection [2], they could manifest themselves at LHC via a rich and varied phenomenology.

This review focuses on the three main classes of ED models with prediction at the TeV scale. The aim of the studies was two-fold: establishing the sensitivity to ED signals using detector simulation and various physics backgrounds, as well as assessing whether enough information could be extracted in order to distinguish ED signatures from other new physics signals.

The studies are based on fast simulation tools which describe accurately the expected detector performance. The relevant aspects of the simulation have been validated [3] in full simulation and with test-beam data whenever possible. Except when stated otherwise, all the results and plots presented here are for an integrated luminosity of  $100 \text{ fb}^{-1}$  collected by one of the experiments (i.e. one year at the nominal luminosity of LHC,  $10^{34} \text{ cm}^{-2}\text{s}^{-1}$ ).

## 2 Large extra dimensions

In this scenario, the SM fields are confined in our 4D world and only gravity propagates in the bulk. The model is characterized by the number of extra dimensions  $\delta$  and by the new fundamental scale  $M_D$ . The graviton expands in 4D into a tower of Kaluza-Klein (KK) excitations which couple universally to all SM fields. Even though this coupling is small ( $1/M_{Pl}$ ), the large number of states and their small mass splitting lead to sizeable cross-sections at the LHC.

The virtual exchange of KK excitations of graviton can lead to deviations in Drell-Yan cross-sections and asymmetries in SM processes. The left plot of Fig. 1 illustrates such deviations in the  $\gamma\gamma$  invariant mass distribution [4].

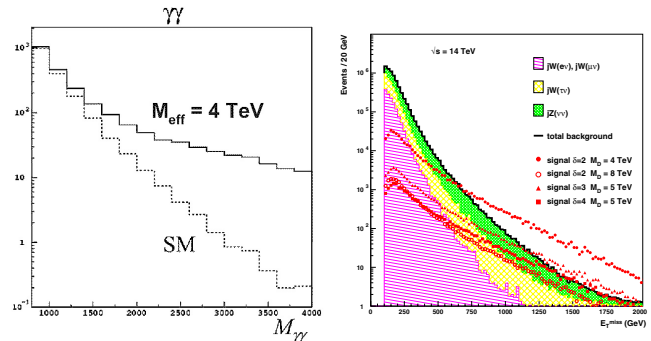


**Fig. 1. Large ED.** Left plot [4]: virtual exchange of gravitons. The plot shows the deviation in Drell-Yan cross-section  $pp \rightarrow \gamma\gamma$  (top curve) with respect to the SM expectation [4]. Right plot [5]: direct production. Missing energy distribution (dots), shown here for various choices of the number of ED ( $\delta$ ) and of the mass scale ( $M_D$ ) and for SM backgrounds (histograms)

This kind of signatures is clear, very sensitive to new physics and could signal the existence of extra dimensions. However the underlying parameters of the model cannot be extracted in this case because the model is sensitive to unknown ultra-violet physics.

The second class of signatures is the direct production of KK excitations of graviton which will escape detection in 4D:  $q\bar{q} \rightarrow gG^{(k)}$ ,  $gq \rightarrow qG^{(k)}$  and  $gg \rightarrow gG^{(k)}$ . In this case, the main signature to look for is some missing energy accompanied by a mono-jet (Fig. 1, right plot) [5]. Within the allowed region for the effective theory ( $\sqrt{\hat{s}} < M_D$ ), those processes can be reliably calculated and the parameters of the model can be constrained from the measurements. Models with up to four extra dimensions could be probed at LHC. For  $100 \text{ fb}^{-1}$ , the maximum reach in  $M_D$  is between 9.1 TeV ( $\delta = 2$ ) and 6.0 TeV ( $\delta = 4$ ), corresponding to a radius of compactification between 8  $\mu\text{m}$  and 1 pm. The two parameters of the model can in principle be extracted from the absolute cross-section of

the processes or more definitely by collecting  $\sim 50 \text{ fb}^{-1}$  of data at a different center-of-mass energy.

### 3 $\text{TeV}^{-1}$ -sized extra dimensions

In this case, the ED are small enough to allow the propagation of gauge bosons in the bulk without contradicting the existing electroweak measurements. Only models with one small ED are considered here, with the fermions localized in the brane at different locations (M1 and M2 models). The main feature of this model is the production of KK excitations of the  $Z$  and  $W$  bosons. Their mass spectrum is defined by:  $m_{Z^{(k)}, W^{(k)}}^2 = m_{Z, W}^2 + k^2 M_C^2$  where  $M_C$  is the compactification scale, known to be  $\geq 4 \text{ TeV}$  from precision electroweak data. Hence only the first excitations  $Z^{(1)}$  and  $W^{(1)}$  can be seen at LHC. In the electron channel [6] the experimental resolution is smaller than the natural width of the  $Z^{(1)}$ . The expected signal<sup>1</sup> is shown on Fig. 2, left plot. The direct observation of a peak is possible if  $M_C \leq 5.8 \text{ TeV}$ . However, this reach can be improved drastically by using all the information with a maximum likelihood, in particular using the region before the peak (Fig. 2, left) with either constructive or destructive interferences between the  $Z^{(1)}/\gamma^{(1)}$  and  $Z/\gamma$ . The sensitivity is thus increased to  $M_C^{\text{max}} = 9.5 \text{ TeV}$  and could even reach  $13.5 \text{ TeV}$  by combining the electron and muon channels for  $300 \text{ fb}^{-1}$ .

Furthermore, the spin-1  $Z^{(1)}$  signal can be distinguished from a spin-2 narrow graviton resonance (Sect. 4) using the angular distribution of its decay products. Thanks to the contributions of the higher lying states, the interference terms and to the additional  $\sqrt{2}$  factor in its coupling to SM fermions, the  $Z^{(1)}$  can also be distinguished from a  $Z'$  with SM-like couplings: the distribution of the forward-backward asymmetry for the various cases are shown on Fig. 2 for 4 TeV resonances. The  $Z^{(1)}$  hypothesis can be discriminated for masses up to about 5 TeV with an integrated luminosity of  $300 \text{ fb}^{-1}$ .

### 4 Warped extra dimensions

We consider here one of the Randall-Sundrum models of warped ED, where gravity propagates in a 5D bulk limited by two branes. The SM fields are confined in the first brane. The metric includes an exponential warp factor which curves the space and connects the  $M_{EW}$  scale in the SM brane to the Planck scale in the other brane, hence reformulating the hierarchy problem. The phenomenology is defined by two parameters: the scale of physical processes in the SM brane,  $\Lambda_\pi \sim 1 \text{ TeV}$ , and the curvature scale  $c = k/M_{Pl}$ . The main feature of this model is the production of KK graviton narrow resonances, whose masses are given by  $m_n = x_n \Lambda_\pi c$  where  $x_n$  are the roots of the  $J_1$  Bessel function. Here again only the first excitation is likely to be seen at LHC, the other modes being suppressed

<sup>1</sup> NB: this plot is at parton level. The simulation study gives similar results.

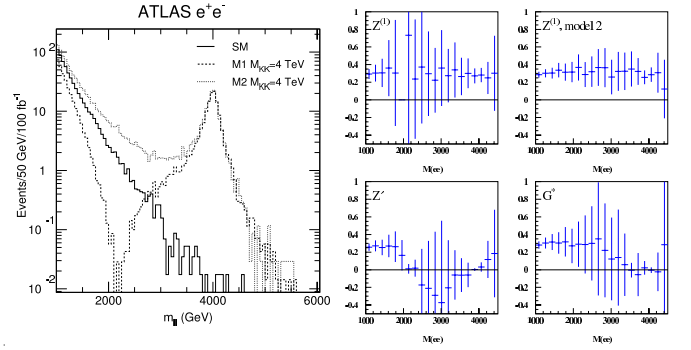


**Fig. 2.  $\text{TeV}^{-1}$ -sized ED.** Left plot [6]: invariant mass distribution of  $e^+e^-$  pairs for the SM (full line) and for two models where  $Z^{(1)}/\gamma^{(1)} \rightarrow e^+e^-$  and  $m_{Z^{(1)}} = 4 \text{ TeV}$ . Right plot [6]: forward-backward asymmetries in the electron channel for different types of resonances, centered at  $m = 4 \text{ TeV}$ : two models for the  $Z^{(1)}$  in  $\text{TeV}^{-1}$  ED models (top), a  $Z'$  (bottom left) and the graviton excitation in RS scenario

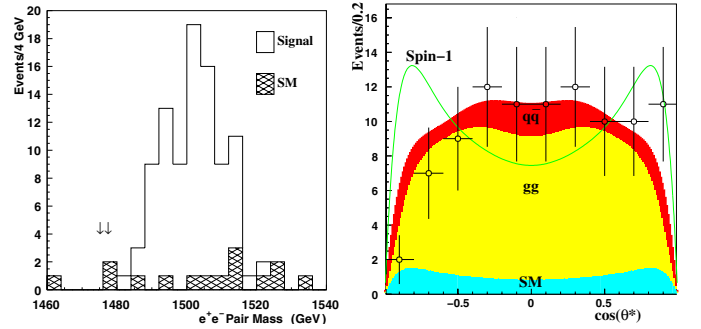


**Fig. 3. Warped ED.** Left plot [7]:  $e^+e^-$  invariant mass distribution from graviton narrow resonance (open histogram) on top of SM background. Right plot [7]: angular distribution of  $e^+e^-$  pairs for the graviton narrow resonance (open circles, yellow curve for the  $gg$  dominant production and red curve for the  $q\bar{q}$  production), for the SM (bottom blue curve) and the expected distribution for a spin 1 resonance (green line)

by the falling parton distribution functions. Some of the best channels are  $G^{(1)} \rightarrow e^+e^-$  and  $G^{(1)} \rightarrow \gamma\gamma$ , thanks to the energy and angular resolutions of the LHC detectors. The signal expected with  $100 \text{ fb}^{-1}$  in the channel  $e^+e^-$  is shown on Fig. 3, left plot, for a pessimistic hypothesis of  $c = 0.01$ . In this case, masses up to 2 TeV can be probed [7]. The reach goes up to about 4 TeV for  $c = 0.1$ . The sensitivity is summarized on Fig. 4 in the  $(m_{G^{(1)}}, c)$  plane [8]: if no signal is found, the area left to the curves labeled "Discovery" can be excluded at 95% CL. The interesting region in this plane is limited by the constraint  $\Lambda_\pi \leq 10 \text{ TeV}$  (otherwise the model would no longer be interesting for solving the hierarchy problem) and by the  $c < 0.1$  limit (low-energy consistency). After one year of data-taking the LHC covers completely this region.

The spin-2 nature of  $G^{(1)}$  can be measured as well as shown on Fig. 3, right plot. It is worth noting that the acceptance at large pseudo-rapidities ( $1.5 < |\eta| < 2.5$ ) is essential for the spin discrimination. The curves labelled "Spin-2" on Fig. 4 show that for graviton masses up to

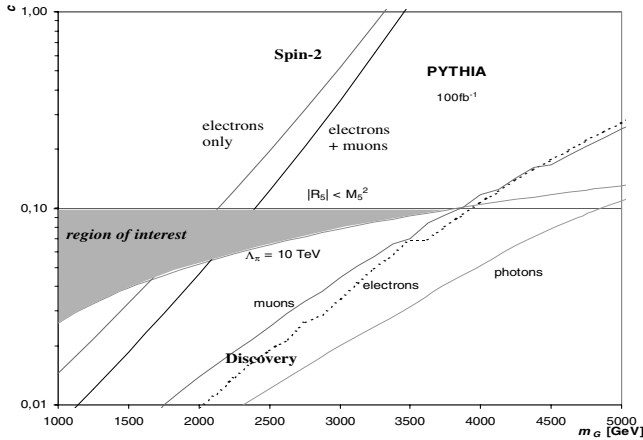


**Fig. 4. Warped ED.** Exclusion limits for discovery of a RS graviton resonance as a function of the mass and of the curvature scale  $c = k/M_{Pl}$ . See text for explanations [8].

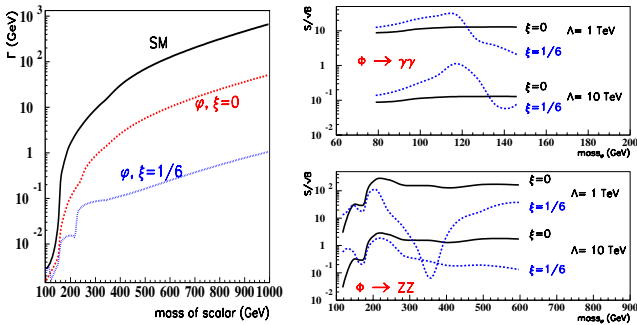


**Fig. 5. Warped ED.** Left plot [9]: width of the radion compared to the one of the SM Higgs. Right plot [9]: significances of two radion decay channels as a function of the radion mass. For  $\xi = 0$  there is no radion-Higgs mixing while for  $\xi = 1/6$  they are heavily mixed

2.3 TeV ( $c = 0.1$ ), there is a 90% chance that the spin-2 nature of the graviton can be determined with a 95% CL. It has also been shown [7] that this resonance can be seen in many other channels ( $\mu\mu, \gamma\gamma, jj, b\bar{b}, t\bar{t}, WW, ZZ$ ), hence allowing to check the universality of its couplings; and that the size  $R$  of the ED could also be estimated with a 10% accuracy from the mass and cross-section measurements.

Another intriguing signature of this model is the existence of a new massive scalar, the radion, allowing to stabilize the spacing between the two branes at the distance required for solving the hierarchy problem ( $kR \sim 12$ ). The radion is very similar to the SM Higgs, and can actually mix with it. Its width is smaller though, as shown on Fig. 5, left plot; and its partial widths can be different, with in particular an enhanced coupling to gluons. There are three additional parameters for the radion: its mass, the vacuum expectation value  $\Lambda_\phi$  and the radion-Higgs mixing parameter  $\xi$ . The results for the SM Higgs have been reinterpreted for the radion case by folding in the new branching ratios and the appropriate detector resolutions [9]. Fig. 5 (right plot) shows the expected signifi-

cances for a radion signal in the  $\gamma\gamma$  and  $ZZ^{(*)}$  channels. Discovery is possible over the whole mass range if  $\Lambda_\phi \sim \text{TeV}$ . If its mass permits, the radion can also decay into a pair of Higgs scalars. If  $m_\phi = 300 \text{ GeV}$ , only  $2(4) \text{ fb}^{-1}$  are needed for a  $5\sigma$  discovery in the very clean channel  $\phi \rightarrow hh \rightarrow \gamma\gamma b\bar{b}$  for  $\xi = 0(1/6)$ . With  $30 \text{ fb}^{-1}$  collected at low luminosity (to maintain excellent  $b$ -tagging), scales up to  $\Lambda_\phi = 2.2 \text{ TeV}$  can be probed in this channel, and up to 1.0 TeV in the  $\phi \rightarrow hh \rightarrow b\bar{b}\tau^+\tau^-$  for  $m_\phi = 600 \text{ GeV}$ . Discrimination between the radion and a Higgs scalar will require very precise measurements of their couplings.

## 5 Other models and signatures

The existence of ED could also be probed with the dijet cross-section [10] or via the polarization of  $\tau$  leptons in some models with two Higgs doublets and a singlet neutrino in the bulk [11]. Finally, the production of black holes at LHC is another striking signature of ED [12].

## 6 Conclusion

The LHC will be able to probe the relevant region of the parameter space for most of the models with ED studied so far. Moreover, in most cases it will be possible to discriminate such signals from other new physics scenarios and infer some information about the underlying model.

*Acknowledgements.* The studies presented here have been performed within the ATLAS and CMS collaborations and as such have made use of tools which are the results of collaboration-wide efforts. I would like to thank in particular G. Azuelos, F. Gianotti, I. Hinchliffe, L. Pape, L. Poggioli, S. Shmatov, P. Traczyk and G. Wrochna.

## References

1. I. Antoniadis, and references therein, these proceedings
2. S. Mele, and references therein, these proceedings
3. see for instance: ATLAS TDR, CERN-LHCC-99-14
4. V. Kabachenko et al., ATLAS Note ATL-PHYS-2001-012
5. L. Vacavant, I. Hinchliffe, *J. Phys. G: Nucl. Part. Phys.* **27**, 1839 (2001)
6. G. Azuelos, G. Polesello, Proc. Les Houches 2001, Physics at TeV Colliders, 210-228 (2001)
7. B.C. Allanach et al., JHEP 9 19 (2000); JHEP 0212 39 (2002)
8. C. Collard et al., CMS Note 2002-050
9. G. Azuelos et al., *Eur. Phys. J. direct* **C4**, 16 (2002)
10. G. Balázs, B. Laforge, hep-ph/0110217 (2001)
11. K. Assamagan, A. Deandrea, *Phys. Rev. D* **65**, 076006 (2002)
12. G. Landsberg, and references therein, these proceedings